Initialization of a Limited Area Model: A Comparison between the Nonlinear Normal Mode and Bounded Derivative Methods

S. J. BIJLSMA AND L. M. HAFKENSCHEID

Royal Netherlands Meteorological Institute, De Bilt, The Netherlands

(Manuscript received 1 August 1985, in final form 18 December 1985)

ABSTRACT

A nonlinear normal mode initialization method is applied to a baroclinic limited area forecast model. This method is very effective in reducing the amplitude of the rapid oscillations during the first hours of the forecast. The results are compared with those using a bounded derivative initialization. The latter method gives equally satisfactory results, requiring less computation than the normal mode method.

1. Introduction

Several methods have been proposed to remove unwanted gravity wave oscillations from a primitive equations forecast model. These methods include the application of the linear and nonlinear balance equation, and dynamic initialization. For a review of this work the reader is referred to Bengtsson (1975). An enormous improvement in initialization was achieved by considering the normal modes of the linearized shallow water equations. This led to the linear normal mode initialization (Williamson, 1976) and nonlinear normal mode initialization (Machenhauer, 1977; Baer, 1977). These methods are based on the fact that for sufficiently large equivalent depths the eigenfunctions of the linearized shallow water equations (Rossby modes, westward and eastward gravity modes) are clearly distinguishable in terms of their frequency (Longuet-Higgins, 1968).

Although these methods were originally formulated for global or hemispheric models (Temperton and Williamson, 1979; Daley, 1979) the nonlinear normal mode initialization method was applied to a limited area model by Brière (1982).

As an alternative to nonlinear normal mode initialization, Browning et al. (1980) proposed the application of the bounded derivative method (Kreiss, 1980), which can be used for the initialization of both global and limited area models. Browning and Kreiss (1982) applied the method to the initialization of the shallow water equations with open boundaries and Semazzi (1985) gives results of its application to the initialization of a barotropic equatorial beta plane model.

The relationship between the two methods, applied to a baroclinic primitive equation model with beta plane geometry, assuming periodic boundary conditions, was investigated by Kasahara (1982).

In this paper we present a nonlinear normal mode method, which is very similar to the method of Brière, and, under appropriate conditions closely related to the method of Bourke and McGregor (1983) and the bounded derivative method.

An outline of the method and its relationship to the method of Brière is given in section 2. In section 3 we formulate the equations for bounded derivative initialization. The relationship of our initialization method to the bounded derivative method and the method of Bourke and McGregor is discussed in section 4. In section 5 we describe some modifications which arise in the initialization of the baroclinic prediction model used in the experiments. Results of the initialization methods discussed in sections 2 and 3 are given in section 6. Conclusions are presented in section 7.

2. Outline of the nonlinear normal mode method

We consider the shallow water equations in differentiated form, on a discrete grid $\lambda_i = \lambda_0 + i\Delta\lambda$, $\theta_j = \theta_0 + j\Delta\theta$, with $M \times N$ interior grid points

$$\frac{\partial}{\partial t}\nabla_a^2\chi(i,j) - f_0\nabla_a^2\psi(i,j) + \nabla_a^2\phi(i,j) = Q_\chi(i,j), \quad (1)$$

$$\frac{\partial}{\partial t}\nabla_a^2\psi(i,j) + f_0\nabla_a^2\chi(i,j) = Q_\psi(i,j), \quad (2)$$

$$\frac{\partial}{\partial t}\phi(i,j) + d\nabla_a^2\chi(i,j) = Q_\phi(i,j), \quad (3)$$

where ϕ is the geopotential, ψ the streamfunction, χ the velocity potential, d the mean free geopotential height and ∇_a^2 the usual five-point discrete Laplacian operator in spherical coordinates λ and θ, denoting longitude and latitude; Q_χ, Q_ψ and Q_ϕ are the nonlinear forcing terms. It is assumed that the Coriolis parameter f_0 is constant, deviations being contained in the nonlinear terms on the right-hand side.

We introduce the (time-independent) functions χ_0, ψ_0 and ϕ_0, which satisfy the discrete Laplace equations

$$\nabla_d^2\chi_0 = 0, \quad \nabla_d^2\psi_0 = 0, \quad \nabla_d^2\phi_0 = 0$$

and are equal to the initial values of χ, ψ and ϕ on the boundary. Then, setting $\chi = \chi_0 + \hat{\chi}$, $\psi = \psi_0 + \hat{\psi}$ and $\phi = \phi_0 + \hat{\phi}$, Eqs. (1)–(3) become

$$\frac{\partial}{\partial t}\nabla_d^2\chi - f_0\nabla_d^2\hat{\psi} + \nabla_d^2\hat{\phi} = Q_\chi, \tag{4}$$

$$\frac{\partial}{\partial t}\nabla_d^2\psi + f_0\nabla_d^2\hat{\chi} = Q_\psi, \tag{5}$$

$$\frac{\partial}{\partial t}\phi + d\nabla_d^2\hat{\chi} = Q_\phi. \tag{6}$$

The normal modes of Eqs. (4)–(6), with the right-hand sides set to zero, can be constructed very easily. Let us write the solution in the form $\hat{\eta}(i,j) = (\hat{\chi}(i,j), \hat{\psi}(i,j), \hat{\phi}(i,j))^T$, where T denotes the transpose, and define the scalar product

$$\langle\hat{\eta}_1, \hat{\eta}_2\rangle = \sum_{i=1}^{M}\sum_{j=1}^{N}[\hat{\phi}_1\hat{\phi}_2^* - d(\hat{\chi}_1\nabla_d^2\hat{\chi}_2^* + \hat{\psi}_1\nabla_d^2\hat{\psi}_2^*)]\cos\theta_j,$$

where the asterisk denotes complex conjugation. Then the normalized Rossby mode and eastward and westward gravity modes are given by [cf. Brière (1982)]

$$\mathbf{P}_{kl1} = \mathbf{A}_{kl1}\sigma_{kl}^{-1}S_{kl}(i,j),$$

$$\mathbf{P}_{klr} = \mathbf{A}_{klr}(\alpha_{kl}\sigma_{kl})^{-1}(2d)^{-1/2}S_{kl}(i,j), \quad r = 2, 3$$

where

$$\mathbf{A}_{kl1} = (0, 1, f_0)^T,$$

$$\mathbf{A}_{klr} = (\nu_{klr}, f_0, -\alpha_{kl}^2 d)^T, \quad r = 2, 3$$

and where $S_{kl}(i,j)$ and $-\alpha_{kl}^2$ are the eigenfunctions and eigenvalues of the discrete Laplacian operator. The Rossby waves are stationary ($\nu_{kl1} = 0$) and $\nu_{kl2} = i\sigma_{kl}$, $\nu_{kl3} = -i\sigma_{kl}$, where $\sigma_{kl} = (\alpha_{kl}^2 d + f_0{}^2)^{1/2}$.

We may expand $\hat{\eta}$ in the normal modes

$$\hat{\eta}(i,j) = \sum_{k=1}^{M}\sum_{l=1}^{N}\sum_{r=1}^{3}\hat{\gamma}_{klr}\mathbf{P}_{klr}$$

where

$$\hat{\gamma}_{klr} = \langle\hat{\eta}, \mathbf{P}_{klr}\rangle.$$

Substituting this into Eqs. (4) to (6) and projection on the gravity modes yields

$$\dot{\gamma}_{klr} = -\nu_{klr}\hat{\gamma}_{klr} + F_{klr}, \quad r = 2, 3$$

where

$$F_{klr} = -(\alpha_{kl}\sigma_{kl})^{-1}(d/2)^{1/2} \times \sum_{i=1}^{M}\sum_{j=1}^{N}[Q_\phi\alpha_{kl}^2 + Q_\chi\nu_{klr}^* + Q_\psi f_0]S_{kl}(i,j)\cos\theta_j,$$

$$\dot{\gamma}_{klr} = -(\alpha_{kl}\sigma_{kl})^{-1}(d/2)^{1/2}\sum_{i=1}^{M}\sum_{j=1}^{N}\left[\frac{\partial\phi}{\partial t}\alpha_{kl}^2 + \frac{\partial}{\partial t}\nabla_d^2\chi\nu_{klr}^* + \frac{\partial}{\partial t}\nabla_d^2\psi f_0\right]S_{kl}(i,j)\cos\theta_j.$$

Following Machenhauer (1977) we set the initial tendencies of gravity wave components to zero, yielding

$$-\nu_{klr}\hat{\gamma}_{klr} + F_{klr} = 0, \quad r = 2, 3.$$

This nonlinear equation can be solved iteratively, as follows:

$$\hat{\gamma}_{klr}^{(q+1)} = F_{klr}^{(q)}/\nu_{klr}, \quad r = 2, 3.$$

The new fields are given by the equations

$$\hat{\eta}^{(q+1)} = \hat{\eta}^{(q)} + \sum_{k=1}^{M}\sum_{l=1}^{N}\sum_{r=2}^{3}(F_{klr}^{(q)}/\nu_{klr} - \hat{\gamma}_{klr}^{(q)})\mathbf{P}_{klr}. \tag{7}$$

These may be used to evaluate $F_{klr}^{(q+1)}$.

In order to point out the difference with the initialization method of Brière (1982), we rewrite (7) as

$$\hat{\eta}^{(q+1)} = \hat{\eta}^{(q)} + \sum_{k=1}^{M}\sum_{l=1}^{N}\sum_{r=2}^{3}(\dot{\gamma}_{klr}^{(q)}/\nu_{klr})\mathbf{P}_{klr}. \tag{8}$$

Let $\hat{\chi}_{kl}$, $\hat{\psi}_{kl}$ and $\hat{\phi}_{kl}$ be the expansion coefficients of $\hat{\chi}$, $\hat{\psi}$ and $\hat{\phi}$ in the normalized eigenfunctions $S_{kl}(i,j)$, e.g.,

$$\hat{\chi}_{kl} = \sum_{i=1}^{M}\sum_{j=1}^{N}\hat{\chi}(i,j)S_{kl}(i,j)\cos\theta_j.$$

Then, using the definition of $\dot{\gamma}$, Eq. (8) may be written as

$$\hat{\chi}_{kl}^{(q+1)} = \hat{\chi}_{kl}^{(q)} - \frac{f_0}{\sigma_{kl}^2\alpha_{kl}^2}\left(\frac{\partial}{\partial t}\nabla_d^2\psi^{(q)}\right)_{kl} - \frac{1}{\sigma_{kl}^2}\left(\frac{\partial\phi^{(q)}}{\partial t}\right)_{kl}, \tag{9}$$

$$\hat{\psi}_{kl}^{(q+1)} = \hat{\psi}_{kl}^{(q)} + \frac{f_0}{\sigma_{kl}^2\alpha_{kl}^2}\left(\frac{\partial}{\partial t}\nabla_d^2\chi^{(q)}\right)_{kl}, \tag{10}$$

$$\hat{\phi}_{kl}^{(q+1)} = \hat{\phi}_{kl}^{(q)} - \frac{d}{\sigma_{kl}^2}\left(\frac{\partial}{\partial t}\nabla_d^2\chi^{(q)}\right)_{kl}, \tag{11}$$

where, for instance,

$$\left(\frac{\partial}{\partial t}\nabla_d^2\chi^{(q)}\right)_{kl} = \sum_{i=1}^{M}\sum_{j=1}^{N}\left(\frac{\partial}{\partial t}\nabla_d^2\chi^{(q)}\right)S_{kl}(i,j)\cos\theta_j.$$

As a result we find that, if (7) converges, the following relations are satisfied:

$$\frac{\partial}{\partial t}\nabla_d^2\chi = 0, \tag{12}$$

$$\frac{\partial}{\partial t}\nabla_d^2(\phi - f_0\psi) = 0. \tag{13}$$

In deriving (13) from (9) we replaced

$$\alpha_{kl}^2\left(\frac{\partial\phi}{\partial t}\right)_{kl} \quad \text{by} \quad -\left(\frac{\partial}{\partial t}\nabla_d^2\phi\right)_{kl}$$

so that the boundary values of $\partial\phi/\partial t$ are not explicitly involved in (13). The initialization method used by Brière [1982, Eqs. (5)–(7)] is in fact the application of (9) to (11). However, he computes the right-hand sides in a different way: the tendencies of divergence and vorticity are obtained from the finite difference analogues of

$$\frac{\partial}{\partial t}\nabla^2\chi = \frac{1}{r\cos\theta}\left[\frac{\partial}{\partial\lambda}u_t + \frac{\partial}{\partial\theta}(v_t\cos\theta)\right],$$

$$\frac{\partial}{\partial t}\nabla^2\psi = \frac{1}{r\cos\theta}\left[\frac{\partial}{\partial\lambda}v_t - \frac{\partial}{\partial\theta}(u_t\cos\theta)\right],$$

where r is the radius of the earth, with the assumption that the tendencies of the zonal and meridional velocity components u and v vanish on the boundary.

3. Derivation of the bounded derivative equations

In order to derive the equations for the bounded derivative method, we consider the shallow water equations in undifferentiated form:

$$\left.\begin{aligned}\frac{\partial u}{\partial t} - f_0 v + \frac{1}{r\cos\theta}\frac{\partial\phi}{\partial\lambda} &= Q_u,\\ \frac{\partial v}{\partial t} + f_0 u + \frac{1}{r}\frac{\partial\phi}{\partial\theta} &= Q_v,\\ \frac{\partial\phi}{\partial t} + \frac{d}{r\cos\theta}\left(\frac{\partial u}{\partial\lambda} + \frac{\partial}{\partial\theta}(v\cos\theta)\right) &= Q_\phi.\end{aligned}\right\}$$

Here d is again the mean free geopotential height. Deviations from the constant Coriolis parameter f_0 are contained in the nonlinear terms Q_u and Q_v. We consider the case without orography. Then, scaling the variables according to Kasahara (1982, p. 386), the scaled equations for the external mode are

$$\left.\begin{aligned}\frac{\partial u}{\partial t} + \epsilon^{-1}\left(\frac{1}{r\cos\theta}\frac{\partial\phi}{\partial\lambda} - f_0 v\right) &= Q_u\\ \frac{\partial v}{\partial t} + \epsilon^{-1}\left(\frac{1}{r}\frac{\partial\phi}{\partial\theta} + f_0 u\right) &= Q_v\\ \frac{\partial\phi}{\partial t} + \epsilon^{-2}\frac{d}{r\cos\theta}\left(\frac{\partial u}{\partial\lambda} + \frac{\partial}{\partial\theta}(v\cos\theta)\right) &= Q_\phi\end{aligned}\right\}, \quad (14)$$

where $d = 1$, $r = 1$ and $\epsilon = O(10^{-1})$. We use the same notation for scaled and unscaled variables. The nonlinear terms are of order unity. Unscaled equations are obtained by setting $\epsilon = 1$.

We apply the bounded derivative method to system (14), i.e., we derive a number of constraints on the initial data by requiring that the time derivatives (to a certain order) of the dependent variables are of order unity at the initial time. The first-order time derivatives are of order unity if

$$\left.\begin{aligned}\frac{1}{r\cos\theta}\frac{\partial\phi}{\partial\lambda} - f_0 v &= \epsilon a\\ \frac{1}{r}\frac{\partial\phi}{\partial\theta} + f_0 u &= \epsilon b\\ \frac{d}{r\cos\theta}\left(\frac{\partial u}{\partial\lambda} + \frac{\partial}{\partial\theta}(v\cos\theta)\right) &= \epsilon^2 c\end{aligned}\right\}, \quad (15)$$

where a, b and c are of order unity. To determine a, b and c we can derive additional equations by requiring that the second-order time derivatives are of order unity. If we assume that the spatial derivatives of $\partial u/\partial t$, $\partial v/\partial t$ and $\partial\phi/\partial t$ are of order unity, the second-order time derivatives are of order unity if $\partial a/\partial t$, $\partial b/\partial t$ and $\partial c/\partial t$ are of order unity. Utilizing (14) and (15), we derive the system of equations

$$\left.\begin{aligned}\epsilon\frac{\partial a}{\partial t} &= \frac{1}{r\cos\theta}\frac{\partial}{\partial\lambda}\left(\frac{\partial\phi}{\partial t}\right) - f_0\frac{\partial v}{\partial t}\\ &= \frac{1}{r\cos\theta}\frac{\partial}{\partial\lambda}(Q_\phi - c) - f_0(Q_v - b)\\ \epsilon\frac{\partial b}{\partial t} &= \frac{1}{r}\frac{\partial}{\partial\theta}\left(\frac{\partial\phi}{\partial t}\right) + f_0\left(\frac{\partial u}{\partial t}\right)\\ &= \frac{1}{r}\frac{\partial}{\partial\theta}(Q_\phi - c) + f_0(Q_u - a)\\ \epsilon^2\frac{\partial c}{\partial t} &= \frac{d}{r\cos\theta}\left[\frac{\partial}{\partial\lambda}\left(\frac{\partial u}{\partial t}\right) + \frac{\partial}{\partial\theta}\left(\frac{\partial v}{\partial t}\cos\theta\right)\right]\\ &= \frac{d}{r\cos\theta}\left[\frac{\partial}{\partial\lambda}(Q_u - a) + \frac{\partial}{\partial\theta}(Q_v\cos\theta - b\cos\theta)\right]\end{aligned}\right\}. \quad (16)$$

We will determine a, b and c only to order unity, i.e., we neglect terms of order ϵ in the nonlinear terms of (16). This leads to the following constraints for a, b and c:

$$\frac{1}{r\cos\theta}\frac{\partial c}{\partial\lambda} - f_0 b = \frac{1}{r\cos\theta}\frac{\partial}{\partial\lambda}Q_\phi - f_0 Q_v, \quad (17)$$

$$\frac{1}{r}\frac{\partial c}{\partial\theta} + f_0 a = \frac{1}{r}\frac{\partial}{\partial\theta}Q_\phi + f_0 Q_u, \quad (18)$$

$$\frac{1}{r\cos\theta}\left[\frac{\partial a}{\partial\lambda} + \frac{\partial}{\partial\theta}(b\cos\theta)\right] = \frac{1}{r\cos\theta}\left[\frac{\partial}{\partial\lambda}Q_u + \frac{\partial}{\partial\theta}(Q_v\cos\theta)\right]. \quad (19)$$

These constraints are not all independent, because (19) can be derived from (17) and (18). However, a third independent relation between a, b and c, derived from (15) is

$$\frac{d}{r\cos\theta}\left(\frac{\partial b}{\partial\lambda} - \frac{\partial}{\partial\theta}(a\cos\theta)\right) = \epsilon f_0 c. \quad (20)$$

Utilizing the first two equations of (15) and observing (19), we obtain

$$\nabla^2\phi - f_0\nabla^2\psi = \frac{\epsilon}{r\cos\theta}\left[\frac{\partial}{\partial\lambda}Q_u + \frac{\partial}{\partial\theta}(Q_v\cos\theta)\right]. \quad (21)$$

Differentiating (17) and (18) with respect to λ and θ, respectively, adding the resulting equations and observing (20), we obtain

$$\nabla^2 c - \frac{\epsilon f_0^2 c}{d} = \nabla^2 Q_\phi + \frac{f_0}{r\cos\theta}\left[\frac{\partial}{\partial\theta}(Q_u\cos\theta) - \frac{\partial}{\partial\lambda}Q_v\right]$$

or, with the third relation of (15)

$$(d\nabla^2 - \epsilon f_0^2)\nabla^2\chi = \epsilon^2\nabla^2 Q_\phi + \frac{\epsilon^2 f_0}{r\cos\theta}\left[\frac{\partial}{\partial\theta}(Q_u\cos\theta) - \frac{\partial}{\partial\lambda}Q_v\right]. \quad (22)$$

Similar equations can be derived for the first internal mode. Equations (21) and (22), in their unscaled form, are

$$\left.\begin{aligned}\nabla^2\phi - f_0\nabla^2\psi &= Q_\chi\\ (d\nabla^2 - f_0^2)\nabla^2\chi &= \nabla^2 Q_\phi - f_0 Q_\psi\end{aligned}\right\}, \quad (23)$$

where the nonlinear terms contain only terms of the highest order. Solving these equations iteratively, we can solve the first equation of (23) for ϕ (or ψ) leaving ψ (or ϕ) unchanged. A better way is to use a simple variational method. Consider the equations

$$\left.\begin{aligned}\nabla^2(\phi^{(q+1)} - f_0\psi^{(q+1)}) &= Q_\chi^{(q)}\\ (d\nabla^2 - f_0^2)\nabla^2\chi^{(q+1)} &= \nabla^2 Q_\phi^{(q)} - f_0 Q_\psi^{(q)}\end{aligned}\right\}. \quad (24)$$

Let Δ denote the difference between two successive iterative solutions of the first equation of (24), i.e.,

$$\Delta = (\phi^{(q+1)} - f_0\psi^{(q+1)}) - (\phi^{(q)} - f_0\psi^{(q)}).$$

Then we consider variations

$$\Delta\phi = \phi^{(q+1)} - \phi^{(q)} \quad \text{and} \quad \Delta\psi = \psi^{(q+1)} - \psi^{(q)},$$

satisfying

$$\Delta\phi - f_0\Delta\psi = \Delta,$$

which minimize

$$(\Delta\phi)^2 + \mu(f_0\Delta\psi)^2, \quad \mu > 0. \quad (25)$$

This leads immediately to

$$\Delta\phi = \mu(1+\mu)^{-1}\Delta \quad \text{and} \quad \Delta\psi = -f_0^{-1}(1+\mu)^{-1}\Delta.$$

The freedom of choice for the value of μ enables us to distribute the changes arbitrarily between the height and wind fields. The effect of the parameter μ on the convergence speed of the iteration process is discussed in section 6d.

4. Relationship between the two methods

Let us consider the iterative procedure from section 2

$$\nu_{klr}\hat{\gamma}_{klr}^{(q+1)} = F_{klr}^{(q)}, \quad r = 2, 3. \quad (26)$$

Using the definitions of ν_{klr}, $\hat{\gamma}_{klr}$ and F_{klr} and equating real and imaginary parts, we note that this relation yields

$$-\alpha_{kl}^2(\hat{\phi}_{kl}^{(q+1)} - f_0\hat{\psi}_{kl}^{(q+1)}) = (Q_\chi^{(q)})_{kl},$$

$$(\alpha_{kl}^2 d + f_0^2)\alpha_{kl}^2\hat{\chi}_{kl}^{(q+1)} = -\alpha_{kl}^2(Q_\phi^{(q)})_{kl} - f_0(Q_\psi^{(q)})_{kl},$$

where, for instance,

$$(Q_\chi^{(q)})_{kl} = \sum_{i=1}^{M}\sum_{j=1}^{N} Q_\chi^{(q)}(i,j)S_{kl}(i,j)\cos\theta_j.$$

Since the functions χ_0, ψ_0 and ϕ_0 satisfy the discrete Laplace equation, these equations are equivalent to

$$\nabla_d^2(\phi^{(q+1)} - f_0\psi^{(q+1)}) = Q_\chi^{(q)}, \quad (27)$$

$$(d\nabla_d^2 - f_0^2)\nabla_d^2\chi^{(q+1)} = \nabla_d^2 Q_\phi^{(q)} - f_0 Q_\psi^{(q)}, \quad (28)$$

if the (unknown) boundary values of Q_ϕ and $\nabla_d^2\chi$ are set to zero. From (10) and (11) it follows that

$$f_0(\phi^{(q+1)} - \phi^{(q)}) = d\nabla_d^2(\psi^{(q+1)} - \psi^{(q)}). \quad (29)$$

Equations (27) and (28), together with relation (29), are, in fact, the equations employed by Bourke and McGregor (1983, condition B). These equations constitute the iterative solution of the discrete analogue of

$$\left.\begin{aligned}\nabla^2(\phi - f_0\psi) &= Q_\chi\\ (d\nabla^2 - f_0^2)\nabla^2\chi &= \nabla^2 Q_\phi - f_0 Q_\psi\end{aligned}\right\}, \quad (30)$$

which are, within the degree of approximations, identical to (23). In the experiments of section 6, Eq. (30) instead of Eq. (23) are used as the bounded derivative equations. From Eqs. (1)–(3) it follows that system (30) is equivalent to [cf. also (12) and (13)]

$$\frac{\partial}{\partial t}\nabla^2\chi = 0,$$

$$\frac{\partial}{\partial t}\nabla^2(\phi - f_0\psi) = 0.$$

Of course, the nonlinear normal mode method has a significant advantage over the bounded derivative method and the method of Bourke and McGregor in that different horizontal scales or time scales may be treated differently. Moreover, changes in wind and height field are related by means of (29), consistent with geostrophic adjustment theory.

However, if it is sufficient to initialize one or two vertical modes, which is the number of modes which can be initialized by the bounded derivative method and if all corresponding gravity wave coefficients are modified according to (26), so that Eqs. (27) and (28) can be derived, then the nonlinear normal mode

method, the method of Bourke and McGregor and the bounded derivative method are very similar.

5. Initialization of the baroclinic model

The prediction model is essentially the limited area version of the ECMWF grid point model employed by Temperton and Williamson (1979). Let Φ_n be defined by

$$\Phi_n = \bar{\phi}_n^{\sigma} + R\bar{T}_n \ln p_s, \quad (n = 1, \cdots, K),$$

where n is the vertical index, $\bar{T}_n = \bar{T}_n(\sigma)$ the mean state temperature, p_s the surface pressure, R the gas constant and $\bar{\phi}_n^{\sigma}$ the vertically averaged geopotential obtained from the vertically summed hydrostatic equation

$$\phi_{n+1/2} = \phi_s + \sum_{l=n+1}^{K} RT_l(\Delta_\sigma \ln\sigma)_l,$$

where ϕ_s is the geopotential height of the earth's surface and Δ_σ the vertical difference operator.

Further, let **E** be the matrix whose columns are the vertical modes with corresponding equivalent geopotential heights d_m ($m = 1, \cdots, K$). [For details the reader is referred to Temperton and Williamson (1979).]

Then, after a vertical transformation, the model equations in differentiated form are equivalent to system (1)–(3) for each vertical mode, if ϕ is replaced by the expansion coefficient of Φ_n for a particular vertical mode; and the initialization procedures described in sections 2 and 3 can be applied for sufficiently large equivalent geopotential height d_m. However, at each iteration step, corrections $\Delta \ln p_s$ and ΔT_n of the surface pressure and temperature fields must be computed from the modification $\Delta\Phi_n$ of Φ_n, obtained from the changes of the expansion coefficients $\Delta\bar{\Phi}_m$ by

$$\Delta\Phi_n = \sum_{j=1}^{K} E_{nj}\Delta\bar{\Phi}_j.$$

This can be done by a method, described by Temperton and Williamson (1979, p. 27), which makes use of the linear continuity equation. Unfortunately, this method did not work very well, especially not over regions with high orography, where the changes in surface pressure appeared to be rather large, while the temperature changes were negligible.

Therefore, we used a variational method, due to Daley (1979). In this method modifications of p_s and T_n are obtained by minimizing

$$\sum_{n=1}^{K} \alpha_n(\Delta T_n)^2(\Delta_\sigma\sigma)_n + \beta(\bar{T}_K\Delta \ln p_s)^2 \qquad (31)$$

with the constraint

$$\Delta\Phi_n = \Delta\bar{\phi}_n^{\sigma} + R\bar{T}_n\Delta \ln p_s.$$

The weights α_n, β are discussed in section 6.

6. Experiments and results

a. *The limited area model*

In order to test the initialization methods described above a number of test runs were made with the limited

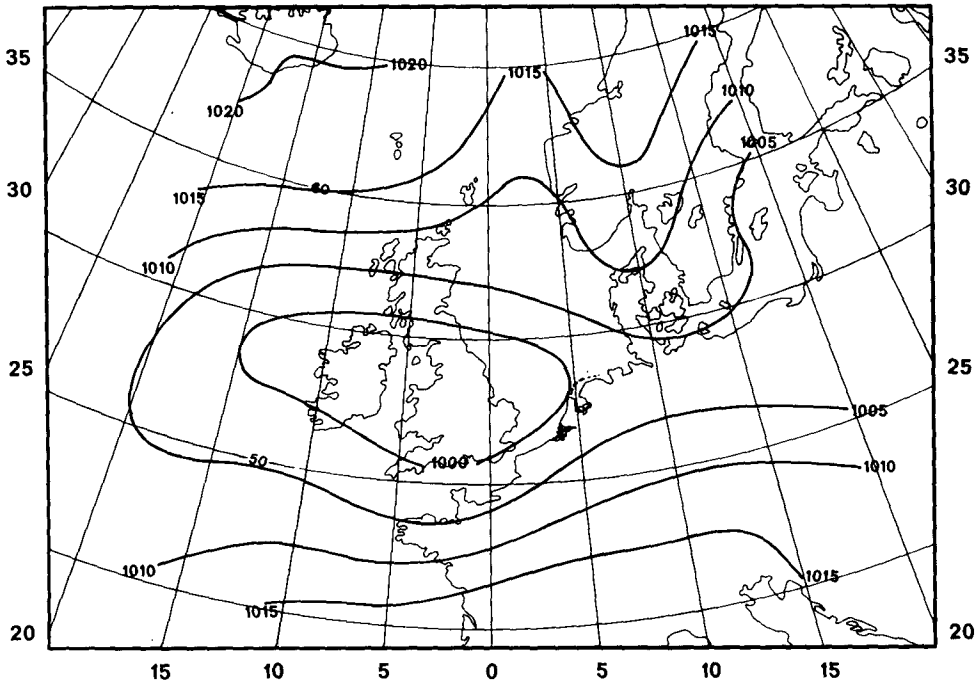

FIG. 1. Uninitialized mean sea level pressure at 1200 GMT 5 January 1982. Units are millibars.

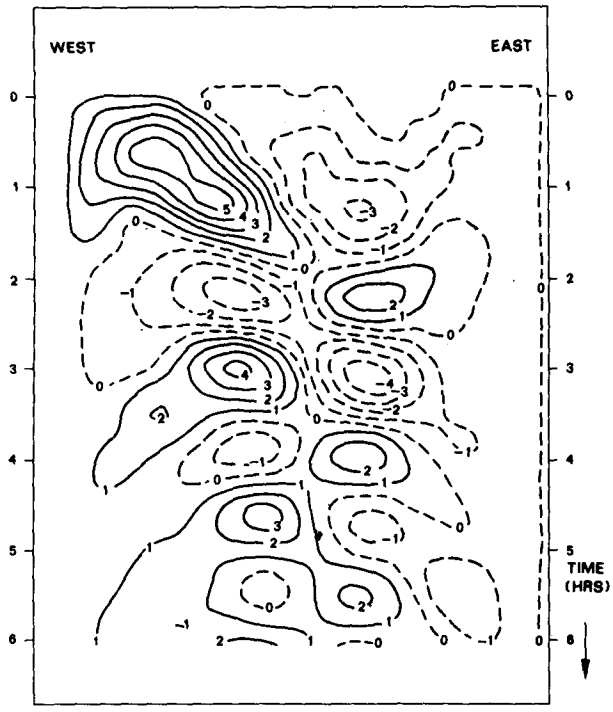

FIG. 2. Longitude–time diagram of surface pressure tendencies along the latitude line of 55°N, starting at 1200 GMT 5 January 1982, before initialization. Units are millibars per hour.

area version of the ECMWF grid point model with Davies boundary conditions (Davies, 1976). This model uses the Arakawa C grid in which the u-points are staggered half a grid point distance to the east and the v-points half a grid point distance to the north with respect to the T-points. The grid was formed by 21 × 22 grid points with a grid point distance of 2.0° in the east–west direction and 1.0° in the north–south direction. The number of levels used is five with sigma values 0.0766, 0.2601, 0.5000, 0.7651 and 0.9666. The test runs were all adiabatic runs with a semi-implicit time step of 15 minutes.

b. Initial data and experiments

Initial data are obtained from analyses of the geopotential at pressure levels. Temperatures are derived hydrostatically. Wind components u and v at sigma levels are calculated with the linear balance equation; orography is included.

Initialization starts with calculating vorticity and divergence on the unstaggered grid points. From vorticity and divergence the streamfunction ψ and velocity potential χ are derived by solving Poisson equations. After initialization, u and v (staggered) are calculated from ψ and χ. For the weight functions α_n and β used to calculate the changes in T and $\ln p_s$ [cf. Eq. (31)], different values were tested. For very small weights of the surface pressure changes, allowing large surface pressure changes and small temperature changes, it appeared that these changes were precisely the same as those obtained by the method of Temperton and Williamson mentioned in section 5. By gradually increasing the weight of the surface pressure changes, an optimal ratio of weights could be found. The effect on the 6-h forecasts by changing the weights was very small. The best choice appeared to be the ratio $\beta:\alpha_n = 1.0:0.1$, giving moderate changes for both surface pressure and temperatures. These values are used in all experiments. Vertical modes were calculated with temperatures from the ICAO standard atmosphere.

The effect of the initialization can be made visible by plotting the surface pressure versus time in a single grid point. A better presentation is given by means of longitude–time diagrams of the surface pressure tendencies along a latitude line; in this paper it is always along 55°N, ranging from 22°W to 20°E.

A set of experiments was performed on initial data 1200 GMT 5 January 1982. The mean sea level pressure is given in Fig. 1, showing a cyclone over the British Isles. In the subsequent 12 hours the cyclone has moved to Poland, followed by an outbreak of cold air over western Europe. Figure 2 shows the longitude–time diagram for the first 6 hours of the limited area model run. The diagram shows the gravity wave pattern before initialization.

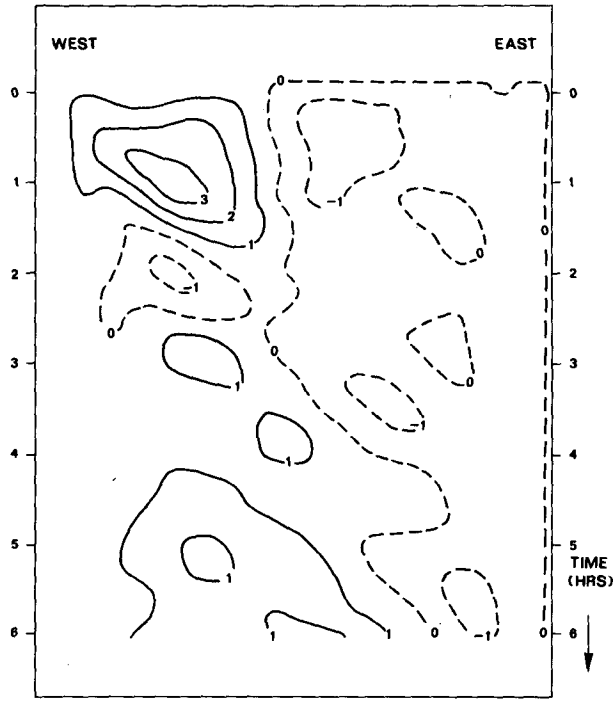

FIG. 3. As in Fig. 2, but after normal mode initialization of the first two vertical modes, with two iterations.

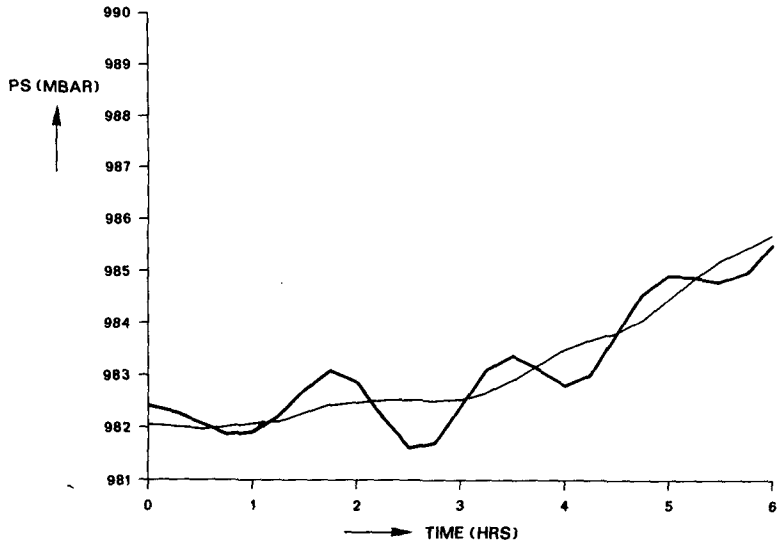

FIG. 4. Surface pressure–time plot for grid point at 55°N, 4°W starting at 1200 GMT 5 January 1982. Before normal mode initialization (heavy line) and after normal mode initialization of two vertical modes with two iterations (thin line).

c. *Results of normal mode initialization*

In Fig. 3 the longitude-time diagram is shown after initialization of the first two vertical modes with two iterations. The substantial reduction of gravity wave amplitudes can also be seen in Fig. 4 which is the surface pressure-time plot of the grid point with coordinates 55°N, 4°W. Figure 5 gives the changes in the mean sea level pressure by this normal mode initialization.

As to the number of iterations and the number of vertical modes to be initialized, it appears that the number of iterations has little effect. The surface pressure tendencies diagram after one iteration (not shown) is almost the same as after two iterations (Fig. 3) and after three iterations (not shown). The number of initialized vertical modes causes slightly larger differences: initializing two vertical modes gives slightly better results than one; initializing the third vertical mode as well gives no improvement.

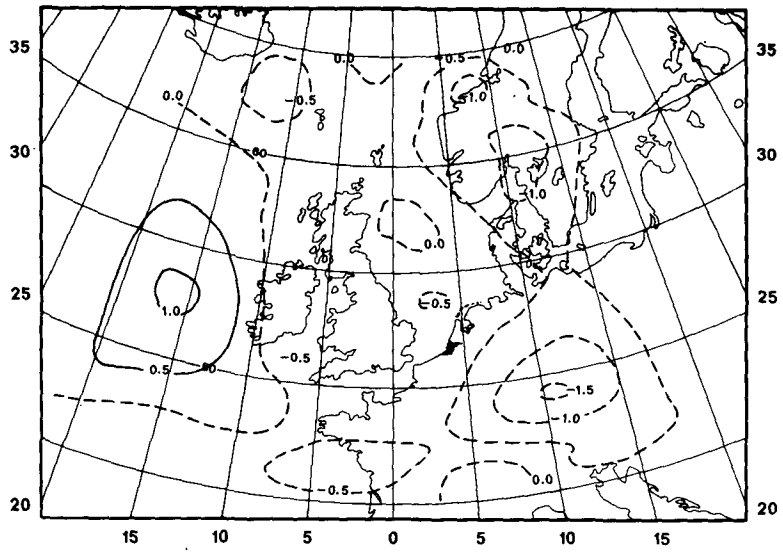

FIG. 5. Mean sea level pressure changes at 1200 GMT 5 January 1982, by initialization of two vertical modes with two iterations. Units are millibars.

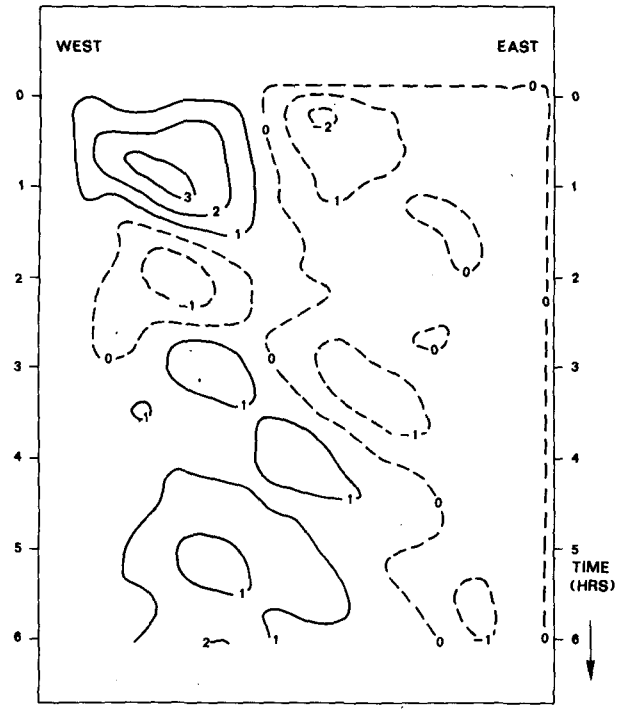

FIG. 6. As in Fig. 3, but after bounded derivative initialization with $\mu = 100$ of the first vertical mode.

d. *Results of the bounded derivative initialization*

The bounded derivative method as described in section 3 was applied to the same initial data as the normal mode method, and subsequently the same model run was made. In this method the changes necessary to achieve the desired initialized state can be spread over the streamfunction ψ and the geopotential Φ with different weights, by means of the coefficient μ in Eq. (25). For small values of μ the main changes are in ψ, with small changes in Φ, and vice versa. The initialization was done for the first vertical mode, and stopped after five iterations. For the coefficient μ, four values were used, namely $\mu = 0.01, 0.5, 2$ and 100. The surface pressure behavior resulting from model runs on the initialized states was in all four cases very similar to the one obtained by the normal mode method. The longitude–time diagram of the surface pressure tendencies for the case $\mu = 100$ is shown in Fig. 6, which is not significantly different from Fig. 3. To show the differences in the initialized states, the changes of 850-mb geopotential and wind speed with respect to the uninitialized state are given for $\mu = 0.5$ (Fig. 7, showing also the direction of the wind changes) and for $\mu = 100$ (Fig. 8). Another consequence of the value of μ is the convergence speed. For $\mu = 100$ the convergence is almost as fast as the normal mode method, and two iterations are sufficient. The convergence becomes slower for decreasing values of μ, but for $\mu = 0.5$ three iterations are still sufficient. For $\mu = 0.01$, however, the procedure did not converge, because for very small values of μ the equations approach a balance equation where, in general, the required ellipticity condition will not be fulfilled [cf. Daley (1978, p. 210) or Kasahara (1982, p. 395)]. The state obtained after five iterations was, nevertheless, close enough to the desired balance to give a surface pressure behavior similar to the one shown in Fig. 6, but after more iterations the result declined away from the solution.

Finally, we inspected the final state resulting from a 6-h model run and compared it with the uninitialized one. As can be seen from Fig. 9, the differences between the final states are smaller than the differences between the initial states. The same holds for the normal mode initialization. The differences between the final states resulting from initialized and uninitialized initial states increase slightly with decreasing values of μ. Therefore, the forecast is not affected by the initialization procedures.

e. *Comparison between the normal mode and the bounded derivative method*

The results of the bounded derivative method are almost identical to the results of the normal mode method. From the four given values of μ the correspondence with the normal mode method was largest for $\mu = 2$, both for the initialized state and for the final state after a 6-h integration. The bounded derivative method has the advantage of possibly altering the ratio of wind field and height field changes. If it is desirable to produce an initialized analysis with small changes in the height field, a smaller value of μ can be chosen (at the cost of convergence speed). This is the case in the example tested here, for which the initial wind field was calculated from a height field analysis. For large values of μ the wind changes are smaller and the height changes larger than those resulting from the normal mode method.

f. *An additional experiment*

The experiments presented so far used initial data for which the wind fields were calculated from the height analyses by means of the linear balance equation. Furthermore, the number of grid points was rather small with a low horizontal resolution. Therefore we will give briefly some results from an experiment with analyzed wind fields and with a grid that is suitable for operational short range forecasting. In this experiment the grid, covering most of western Europe, contained 46×50 grid points with a grid point distance of 0.55° (ca. 60 km), and 11 levels in the vertical. The initial fields were analyzed with a multivariate three-dimensional optimum interpolation scheme, and initialized with the nonlinear normal mode initialization de-

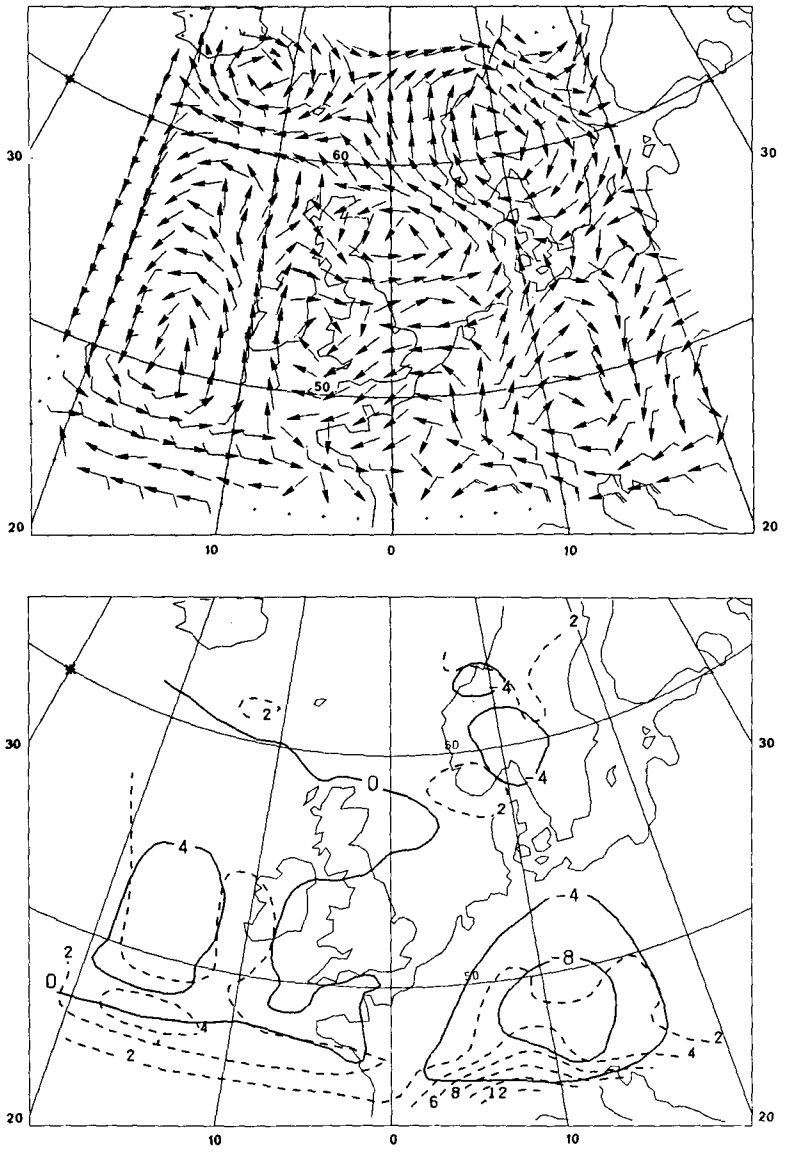

FIG. 7. Changes of 850-mb geopotential (geopotential meters) and wind speed (meters per sec; dashed lines) due to bounded derivative initialization with $\mu = 0.5$. Upper part: 850-mb wind changes in the form of wind shafts.

scribed in this paper. Two vertical modes were initialized with two iterations. With this system a number of analyses and forecast runs were made starting at 1200 GMT 11 May 1983, and with an update frequency of three hours. Although this experiment was not especially set up as an initialization experiment, it is interesting to see how the initialization behaves under these circumstances.

The initialization appeared to be very satisfactory, as can be seen from Fig. 10. This figure shows a surface pressure-time plot for a grid point in the center of the area. The analysis time for this case was 1200 GMT 11 May 1983. Differences in surface pressure between initialized and uninitialized model runs, initially with values up to 3 mb, had disappeared almost completely after about nine hours integration. Another interesting result concerns the precipitation amounts calculated with diabatic model runs. The hourly precipitation amounts during the first hours of a forecast were practically the same as the amounts for the same period resulting from model runs starting at earlier analysis times. These amounts (up to approximately 3 mm per hour during three hours) agreed very well with observations. So the initialization had no negative effect on the predicted precipitation amounts, not even in the first three hours of the forecast.

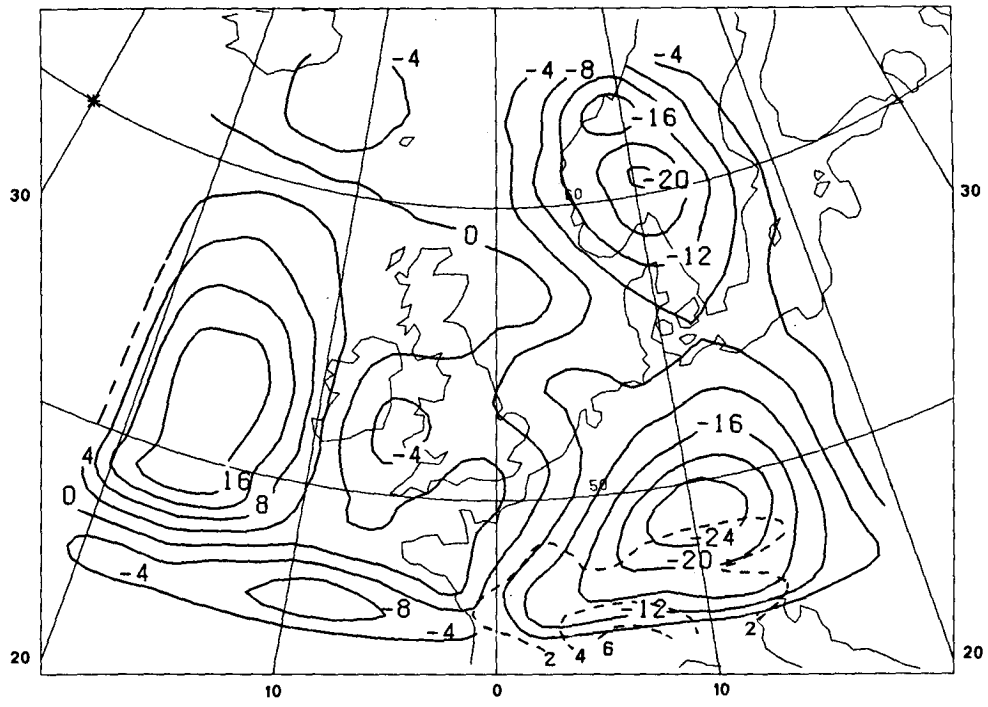

FIG. 8. As in Fig. 7, lower part, but for $\mu = 100$.

7. Conclusions

Results of a number of experiments with both the nonlinear normal mode and the bounded derivative initialization method have been presented. The two methods are virtually identical in their effect upon the initial fields, and both are successful in removing the high frequency oscillations during early forecast hours.

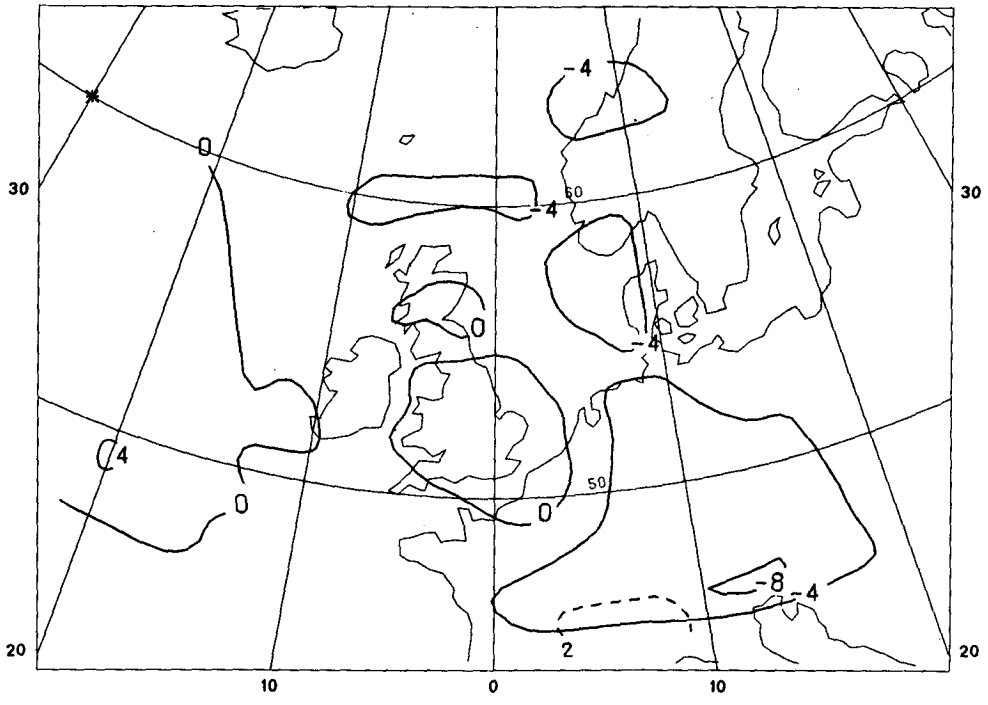

FIG. 9. Differences of 850-mb geopotential and wind speed between a 6-h forecast on data initialized with the bounded derivative method with $\mu = 100$ and a 6-h forecast on uninitialized data. Legend as in Figs. 7 and 8.

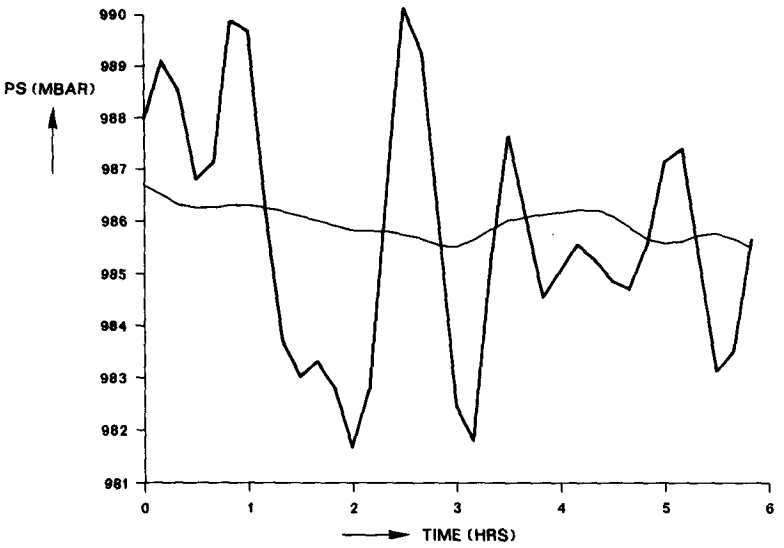

FIG. 10. Surface pressure–time plot of two model runs with analyzed initial wind fields on a fine mesh, starting at 1200 GMT 11 May 1983. Without initialization (heavy line) and with normal mode initialization of two vertical modes with two iterations (thin line).

However, if no special requirements are to be imposed upon the initialized analysis, a variational version of the bounded derivative method allowing small changes in the streamfunction would appear the more attractive one, as it requires less computation.

Acknowledgments. The authors would like to thank Dr. P. Lynch for helpful comments and suggestions.

REFERENCES

Baer, F., 1977: Adjustment of initial conditions required to suppress gravity oscillations in nonlinear flows. *Beitr. Phys. Atmos.*, **50**, 350–366.

Bengtsson, L., 1975: Four-dimensional assimilation of meteorological observations. WMO/ICSU Joint Organizing Committee, Garp Publications Series No. 15, 76 pp. [Case postale No. 5, CH-1211 Geneva 20, Switzerland.]

Bourke, W., and J. L. McGregor, 1983: A nonlinear vertical mode initialization scheme for a limited area prediction model. *Mon. Wea. Rev.*, **111**, 2285–2297.

Brière, S., 1982: Nonlinear normal mode initialization of a limited area model. *Mon. Wea. Rev.*, **110**, 1166–1186.

Browning, G., and H.-O. Kreiss, 1982: Initialization of the shallow water equations with open boundaries by the bounded derivative method. *Tellus*, **34**, 334–351.

——, A. Kasahara and H.-O. Kreiss, 1980: Initialization of the primitive equations by the bounded derivative method. *J. Atmos. Sci.*, **37**, 1424–1436.

Daley, R., 1978: Variational nonlinear normal mode initialization. *Tellus*, **30**, 201–218.

——, 1979: The application of nonlinear normal mode initialization to an operational forecast model. *Atmos. Ocean*, **17**, 97–124.

Davies, H. C., 1976: A lateral boundary formulation for multi-level prediction models. *Quart. J. Roy. Meteor. Soc.*, **102**, 405–418.

Kasahara, A., 1982: Nonlinear normal mode initialization and the bounded derivative method. *Rev. Geophys. Space Phys.*, **20**, 385–397.

Kreiss, H.-O., 1980: Problems with different time scales for partial differential equations. *Commun. Pure Appl. Math.*, **33**, 399–440.

Longuet-Higgins, M. S., 1968: The eigenfunctions of Laplace's tidal equations over a sphere. *Phil. Trans. Roy. Soc., London*, **A262**, 511–607.

Machenhauer, B., 1977: On the dynamics of gravity oscillations in a shallow water model, with applications to normal mode initialization. *Beitr. Phys. Atmos.*, **50**, 253–271.

Semazzi, F. H. M., 1985: An investigation of the equatorial orographic-dynamic mechanism. *J. Atmos. Sci.*, **42**, 78–83.

Temperton, C., and D. L. Williamson, 1979: Normal mode initialization for a multi-level grid point model. European Centre for Medium Range Weather Forecasts, Tech. Rep. No. 11, 91 pp. [Shinfield Park, Reading, Berkshire RG2 9AX, England.]

Williamson, D. L., 1976: Normal mode initialization procedure applied to forecasts with the global shallow water equations. *Mon. Wea. Rev.*, **104**, 195–206.